Mass Transport in the Stokes Edge Wave for Constant Arbitrary Bottom Slope in a Rotating Ocean

PEYGHAM GHAFFARI AND JAN ERIK H. WEBER

Department of Geosciences, University of Oslo, Oslo, Norway

ABSTRACT

The Lagrangian mass transport in the Stokes surface edge wave is obtained from the vertically integrated equations of momentum and mass in a viscous rotating ocean, correct to the second order in wave steepness. The analysis is valid for bottom slope angles β in the interval $0 < \beta \leq \pi/2$. Vertically averaged drift currents are obtained by dividing the fluxes by the local depth. The Lagrangian mean current is composed of a Stokes drift (inherent in the waves) plus a mean Eulerian drift current. The latter arises as a balance between the radiation stresses, the Coriolis force, and bottom friction. Analytical solutions for the mean Eulerian current are obtained in the form of exponential integrals. The relative importance of the Stokes drift to the Eulerian current in their contribution to the Lagrangian drift velocity is investigated in detail. For the given wavelength, the Eulerian current dominates for medium and large values of β, while for moderate and small β, the Stokes drift yields the main contribution to the Lagrangian drift. Because most natural beaches are characterized by moderate or small slopes, one may only calculate the Stokes drift in order to assess the mean drift of pollution and suspended material in the Stokes edge wave. The main future application of the results for large β appears to be for comparison with laboratory experiments in rotating tanks.

1. Introduction

In recent years the interest in coastally trapped waves, for example, the Stokes edge wave, has risen considerably. This is particularly so because they have been shown to be of fundamental importance in the dynamics and the sedimentology of the nearshore zone through their interaction with ocean swell and surf to produce rip current patterns, beach cusps, and crescentic bars (LeBlond and Mysak 1978). The nonlinear mean mass transport in such waves has also been investigated, for example, Weber and Ghaffari (2009) for a nonrotating ocean, where a comprehensive list of references to earlier works in a homogeneous ocean can be found. The edge wave problem has also been carried on to a stratified ocean (Greenspan 1970). A thorough discussion of the linear edge wave problem in a rotating ocean with continuous stratification can be found in Llewellyn Smith (2004). Finally, the nonlinear wave drift in interfacial edge waves in a rotating viscous ocean has been investigated by Weber and Støylen (2011), using a shallow-water approach.

For a rotating ocean, Johns (1965) discovered that trapped edge waves with frequency ω are restricted to slopes such that $\cos\beta > f/\omega$, where β is the bottom slope angle and f is the constant Coriolis parameter. In the case of Johns, waves traveled northward along a western boundary. For edge waves propagating with the coast to the right in the Northern Hemisphere, there is no restriction on the slope (Weber 2012). In the limit where the sloping bottom becomes a vertical wall, the edge wave becomes a geostrophically balanced Kelvin wave.

In the present study, we focus on the mean Lagrangian mass transport induced by the Stokes edge wave. It is this transport that advects neutral tracers and bottom sediment in suspension along the shore in the region of wave trapping. To obtain a robust formulation, we consider the vertically integrated equations of momentum and mass (e.g., Phillips 1977) and derive the mean Lagrangian mass transport to second order in wave steepness. The vertically averaged drift current is obtained by dividing the volume flux by the local depth.

Corresponding author address: Peygham Ghaffari, Department of Geosciences, University of Oslo, P.O. Box 1022, Blindern, 0315 Oslo, Norway.
E-mail: peygham.ghaffari@geo.uio.no

The total Lagrangian drift current can be written as the sum of the Stokes drift (Stokes 1847) and a mean Eulerian current (see, e.g., Longuet-Higgins 1953). In the present paper the Eulerian current arises as a balance between the radiation stresses, the Coriolis force, and bottom friction. Earlier, Kenyon (1969) considered the pure Stokes drift in inviscid nonrotating edge waves by applying the hydrostatic approximation, which is valid for small slope angles. However, the Stokes drift and the Eulerian mean current depend on the slope angle in different ways, so we need a formulation that is valid for arbitrary slopes in order to determine their relative importance for a given β to the Lagrangian drift current. This constitutes the main aim of the present paper.

2. Mathematical formulation

We consider trapped surface gravity waves in a homogeneous incompressible fluid with a linearly sloping bottom. The motion is described in a Cartesian system, where the x axis is situated at the undisturbed surface and directed toward the semi-infinite sea, the y axis is directed along the shoreline, and the vertical z axis is positive upward; see the sketch in Fig. 1. The corresponding velocity components are (u, v, and w). Furthermore, the pressure is p and the constant density is ρ. The bottom is given by $z = -h = -x\tan\beta$, where $\beta(\leq\pi/2)$ is the slope angle, and the free surface displacement by $z = \eta$. Here, η is the surface elevation and h is the undisturbed ocean depth. At the free surface, the pressure is constant. The system rotates about the z axis with constant angular velocity $f/2$.

We denote periodic wave variables by a tilde, and the mean flow (averaged over the wave period) is denoted by an overbar. Mean horizontal volume fluxes ($\overline{U}$, $\overline{V}$) are defined by

$$\overline{U} = \overline{\int_{-h}^{\eta} u\,dz} \quad \text{and} \quad \overline{V} = \overline{\int_{-h}^{\eta} v\,dz}. \qquad (1)$$

These are actually the Lagrangian fluxes, because we integrate between material boundaries (Phillips 1977; Weber et al. 2006). By neglecting the effect of friction in
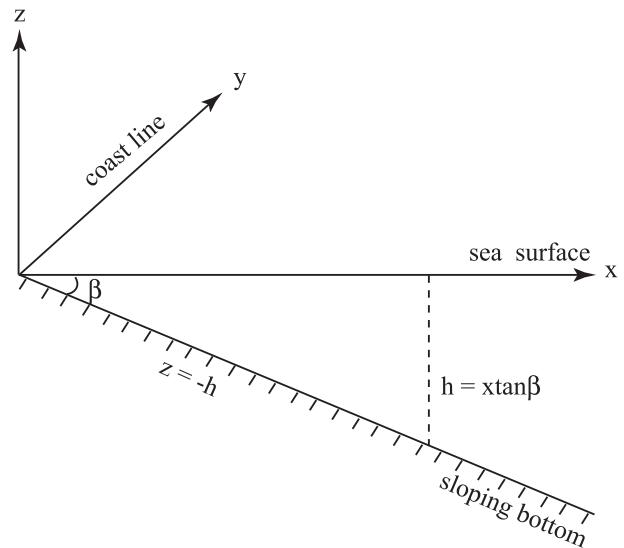

FIG. 1. Sketch depicting the coordinate system, with the surface and sloping bottom included.

the vertical component of the momentum equation, Phillips (1977) found for the mean pressure, correct to second order in wave steepness, that

$$\frac{\overline{p}}{\rho} = g(\overline{\eta} - z) + \frac{\overline{p}_d}{\rho}. \qquad (2)$$

Here $\overline{p}_d$ is the nonhydrostatic (dynamic) part given by

$$\frac{\overline{p}_d}{\rho} = -\overline{\tilde{w}^2} + \frac{\partial}{\partial x}\int_z^0 \overline{\tilde{u}\tilde{w}}\,d\xi + \frac{\partial}{\partial y}\int_z^0 \overline{\tilde{v}\tilde{w}}\,d\xi, \qquad (3)$$

and g is the acceleration due to gravity. It is implicit here that the wave (tilde) quantities are represented by the real parts in a complex formulation. Integrating the governing equations in the vertical, and utilizing the full nonlinear boundary conditions at the free surface and the sloping bottom, we obtain for the mean quantities, correct to second order in wave steepness (Phillips 1977):

$$\frac{\partial \overline{U}}{\partial t} - f\overline{V} + gh\frac{\partial\overline{\eta}}{\partial x} = -\frac{\partial}{\partial x}\int_{-h}^0 \frac{\overline{p}_d}{\rho}\,dz - \frac{g}{2}\frac{\partial}{\partial x}\overline{\tilde{\eta}^2} + \frac{\overline{p}_d(-h)}{\rho}\tan\beta - \frac{\partial}{\partial x}\int_{-h}^0 \overline{\tilde{u}\tilde{u}}\,dz - \frac{\partial}{\partial y}\int_{-h}^0 \overline{\tilde{u}\tilde{v}}\,dz - \tau_1,$$

$$\frac{\partial \overline{V}}{\partial t} + f\overline{U} + gh\frac{\partial\overline{\eta}}{\partial y} = -\frac{\partial}{\partial y}\int_{-h}^0 \frac{\overline{p}_d}{\rho}\,dz - \frac{g}{2}\frac{\partial}{\partial y}\overline{\tilde{\eta}^2} - \frac{\partial}{\partial x}\int_{-h}^0 \overline{\tilde{u}\tilde{v}}\,dz - \frac{\partial}{\partial y}\int_{-h}^0 \overline{\tilde{v}\tilde{v}}\,dz - \tau_2, \quad \text{and} \quad \frac{\partial\overline{\eta}}{\partial t} = -\frac{\partial\overline{U}}{\partial x} - \frac{\partial\overline{V}}{\partial y}. \quad (4)$$

Here

$$\tau_1 \equiv \left.\frac{\overline{\tau}^{(x)}}{\rho}\right|_{-h} \quad \text{and} \quad \tau_2 \equiv \left.\frac{\overline{\tau}^{(y)}}{\rho}\right|_{-h} \tag{5}$$

are the mean turbulent bottom stress components per unit density in the x and y directions, respectively. Their explicit form will be specified later on.

As shown by Mei (1973) for the Stokes standing edge wave, the mean bottom pressure term in the x momentum of (4) $\overline{p}_d(-h)\tan\beta/\rho$, which is missing from Phillips' derivation, must be present here (see also Weber and Ghaffari 2009).

3. Linear waves

In this problem, the oscillatory wave motion is influenced by viscosity acting in thin boundary layers at the surface and at the bottom. Denoting the kinematic viscosity by ν, the boundary layer thickness δ in a nonrotating ocean becomes $\delta = (2\nu/|\omega|)^{1/2}$ (Longuet-Higgins 1953). In a turbulent ocean, ν is the eddy viscosity and may take different values in the top and bottom boundary layers. For shallow-water waves of the tidal type, there are two bottom layers $\delta = (2\nu/|\omega \pm f|)^{1/2}$ associated with the cyclonic and anticyclonic component of the solution (Sverdrup 1927). Within the top and bottom boundary layers the wave velocity varies rapidly with height, while in the interior the variation is that of inviscid waves. The only effect of friction here is that the wave amplitude varies slowly in time or space due to the boundary condition coupling (no surface stress, no-slip bottom) with the boundary layer solutions. In this analysis, we assume that the boundary layers are thin (i.e., $\delta \ll h$). Hence, in the integrals of the wave-forcing terms (with a tilde) in (4), the contributions from the boundary layer parts of the wave velocity can be neglected, and we use the inviscid part of the solution (with a damped amplitude) (see, e.g., Weber et al. 2009). In shallow water with a no-slip bottom, the bottom boundary layer dominates in determining the damping rate. For a nonrotating ocean, this yields a temporal damping rate $(2\nu|\omega|)^{1/2}/(4h)$. In a deep ocean the corresponding damping rate becomes $2\nu k^2$, where k is the wavenumber. In both cases the correct attenuation of the interior motion is obtained by replacing the viscous term $\nu\nabla^2\tilde{\mathbf{u}}$ by $-r\tilde{\mathbf{u}}$ in the linearized momentum equation, where ∇ is the gradient operator and $\tilde{\mathbf{u}} = (\tilde{u}, \tilde{v}, \tilde{w})$ is the linear wave velocity in the interior. Here the friction coefficient r can be related to ν for the case in question. Classifications like deep or shallow water depend on the value of λ/h, where λ is the wavelength. Hence, for a given wavelength, the Stokes edge wave at a certain distance offshore may be characterized as a shallow-water wave for small slope angles,

while for large slopes the same wave may be a deep-water wave (here we investigate slope angles in the interval $0 < \beta \le \pi/2$). We have therefore resorted to an averaging procedure for calculating the damping rate of such waves for all admissible β. A physically appealing and robust formulation is obtained through the calculation the total wave energy E and the total dissipation rate D in the trapped region. Then, the damping rate is determined by $dE/dt = -D$ (see, e.g., Phillips 1977). We return to the detailed calculations in section 4. By adopting the approach outlined above, the linearized equations for the damped interior wave motion become

$$\tilde{u}_t - f\tilde{v} = -\frac{1}{\rho}\tilde{p}_x - r\tilde{u},$$

$$\tilde{v}_t + f\tilde{u} = -\frac{1}{\rho}\tilde{p}_y - r\tilde{v},$$

$$\tilde{w}_t = -\frac{1}{\rho}\tilde{p}_z - g - r\tilde{w}, \tag{6}$$

and

$$\tilde{u}_x + \tilde{v}_y + \tilde{w}_z = 0. \tag{7}$$

Here subscripts denote partial differentiation. The effect of friction on the wave motion is taken to be small. More precisely, we assume that

$$\frac{r}{|\omega|} \ll 1. \tag{8}$$

By applying the curl and the divergence on (6), utilizing (7), the velocity components are easily eliminated. We then find for $\tilde{p}$ that

$$(\partial/\partial t + r)^2 \nabla^2 \tilde{p} + f^2 \tilde{p}_{zz} = 0. \tag{9}$$

We consider surface waves that are trapped at the coast, that is,

$$\tilde{\eta} = \eta_0 \exp[-ax + i(\kappa y - \omega t)], \tag{10}$$

where $\Re(a) > 0$ for the complex parameter a, and η_0 is an arbitrary constant. Furthermore, ω is the wave frequency, and κ is the wavenumber in the y direction (along the coast). The dynamic boundary condition in this problem becomes

$$\tilde{p} = p_0 \quad \text{and} \quad z = \tilde{\eta}. \tag{11}$$

We then infer from (10) and (11) that the pressure in the linear case can be written (Johns 1965)

$$\tilde{p} = p_0 - \rho g z + \rho g \eta_0 \exp[-ax + bz + i(\kappa y - \omega t)], \tag{12}$$

where b is a complex parameter. Inserting (12) into (6), we obtain

$$\tilde{u} = \frac{g\eta_0[-ra + i(\omega a + f\kappa)]}{\omega^2 - f^2 + 2i\omega r} \exp[-ax + bz + i(\kappa y - \omega t)], \tag{13}$$

$$\tilde{v} = \frac{g\eta_0(\omega\kappa + fa + i\kappa r)}{\omega^2 - f^2 + 2i\omega r} \exp[-ax + bz + i(\kappa y - \omega t)], \tag{14}$$

$$\tilde{w} = -\frac{g\eta_0 b}{r - i\omega} \exp[-ax + bz + i(\kappa y - \omega t)]. \tag{15}$$

The kinematic boundary conditions for the linear problem are

$$\tilde{w} = \tilde{\eta}_t \quad \text{and} \quad z = 0, \tag{16}$$

and

$$\tilde{w} = -\tilde{u}\tan\beta \quad \text{and} \quad z = -x\tan\beta. \tag{17}$$

In this analysis we take that the frequency is ω real, while the wavenumber is complex; that is, we consider spatially damped waves. Then we can write

$$\begin{aligned} \kappa &= k + i\alpha, \\ a &= a_r + ia_i, \quad \text{and} \\ b &= b_r + ib_i, \end{aligned} \tag{18}$$

where subscripts r and i denote real and imaginary parts, and α is the spatial damping rate. Trapping at the coast requires $a_r > 0$. In this analysis the parameters α, a_i, and b_i are related to the effect of friction. We show in appendix A that they all are proportional to the small parameter r [see (8)]. Hence, in a nondimensional formulation $k\alpha \ll 1$, $ka_i \ll 1$, and $kb_i \ll 1$. In this problem, we assume that the wavenumber k along the coast is given. The three complex equations of (9), (16), and (17) are sufficient to determine the friction-independent parameters ω, a_r, and b_r and the small friction-related quantities α, a_i, and b_i. In this calculation we neglect squares or products of the small quantities r, α, a_i, and b_i. The effects of rotation and friction will appear through the nondimensional parameters Ω and R, defined by

$$\Omega = \frac{f}{\omega} \quad \text{and} \quad R = \frac{r}{\omega}, \tag{19}$$

where Ω is of the order of unity, and R is small [see (8)]. The calculations of ω, a_r, b_r and α, a_i, and b_i are straightforward, but somewhat time consuming. Therefore, we defer the details to appendix A.

To calculate the mean quantities in (3) and (4), we need real values of our wave solutions. Defining the exponential decay q and the phase function θ by

$$\begin{aligned} q &= -a_r x - \alpha y + b_r z \quad \text{and} \\ \theta &= -a_i x + ky + b_i z - \omega t, \end{aligned} \tag{20}$$

we can write the real part of the surface elevation

$$\tilde{\eta} = \eta_0 \exp q_0 \cos\theta_0, \tag{21}$$

where $q_0 = q|_{z=0}$, $\theta_0 = \theta|_{z=0}$. The real part of the pressure becomes

$$\tilde{p} = p_0 - \rho g z + \rho g \eta_0 \exp q \cos\theta. \tag{22}$$

The velocity components (13)–(15) can be simplified by using the expressions for α, a, and b derived in appendix A. We obtain for the real parts after some algebra:

$$\tilde{u} = -\frac{gk\eta_0 \cos\beta}{\omega(1 - \Omega\cos\beta)} \exp q \sin\theta, \tag{23}$$

$$\tilde{v} = \frac{gk\eta_0}{\omega(1 - \Omega\cos\beta)} \exp q \cos\theta, \quad \text{and} \tag{24}$$

$$\tilde{w} = \frac{gk\eta_0 \sin\beta}{\omega(1 - \Omega\cos\beta)} \exp q \sin\theta. \tag{25}$$

We note from (A16) that $1 - \Omega\cos\beta$ is always positive. It is easily seen from (23) and (25) that $\tilde{w} = -\tilde{u}\tan\beta$ for all q, θ, which shows that the wave motion in the Stokes edge wave occurs in planes parallel to the sloping bottom. This has been utilized by Weber (2012) to find the exact solutions for the Stokes edge wave in a rotating inviscid ocean in Lagrangian coordinates.

4. The damping rate

As mentioned in section 3, we use the formulation of Phillips (1977) to relate the friction coefficient r to the eddy viscosity ν. We find for the total mean energy density that

$$\begin{aligned} E &= \int_0^\infty \left[\int_{-h}^0 \overline{\frac{\rho}{2}(\tilde{u}^2 + \tilde{v}^2 + \tilde{w}^2)}\, dz + \rho g \overline{\int_0^{\tilde{\eta}} z\, dz} \right] dx \\ &= \frac{\rho g \eta_0^2}{8k} \left(\frac{2 - \Omega\cos\beta}{\cos\beta - \Omega} \right) \exp(-2\alpha y). \end{aligned} \tag{26}$$

The total dissipation rate in this problem is readily found to be

$$D = \rho\nu\int_0^\infty \left\{ \int_{-h}^0 \left[\overline{\left(\frac{\partial\tilde{\mathbf{u}}}{\partial x}\right)^2} + \overline{\left(\frac{\partial\tilde{\mathbf{u}}}{\partial y}\right)^2} + \overline{\left(\frac{\partial\tilde{\mathbf{u}}}{\partial z}\right)^2} \right] dz \right\} dx$$

$$= \frac{\rho\nu g k\eta_0^2}{4} \left[\frac{2(1 - \Omega\cos\beta)^2 + \Omega^2\sin^2\beta}{(\cos\beta - \Omega)(1 - \Omega\cos\beta)^2} \right] \exp(-2\alpha y). \tag{27}$$

Here, ν is the bulk eddy viscosity in the fluid. For time-damped waves, we must have $dE/dt = -D$ (Phillips 1977). From Gaster (1962) we know that the transition from temporal to spatial damping is obtained through $d/dt \rightarrow c_g d/dy$, where $c_g = d\omega/dk$ is the group velocity. Hence, for the present problem

$$c_g dE/dy = -D. \tag{28}$$

From (A15), we obtain that

$$c_g = \frac{g\sin\beta}{\omega(2 - \Omega\cos\beta)}. \tag{29}$$

Then, from (26) to (29), we find that the spatial attenuation coefficient is related to the eddy viscosity through

$$\alpha = \left(\frac{\nu k^3}{\omega}\right) \frac{[2(1 - \Omega\cos\beta)^2 + \Omega^2\sin^2\beta]}{(1 - \Omega\cos\beta)^3}. \tag{30}$$

Utilizing (A16), we find

$$\alpha = \frac{2\nu k^2\omega}{g\sin\beta} \left[1 + \frac{1}{2}\left(\frac{f\omega}{gk}\right)^2 \right]. \tag{31}$$

For the nonrotating case ($f = 0$), we recover the result $\alpha = 2\nu k^3/\omega$ from Weber and Ghaffari (2009). The friction coefficient for the linear problem is obtained from (31) and (A21):

$$r = 2\nu k^2 \left[1 + \frac{1}{2}\left(\frac{f\omega}{gk}\right)^2 \right]. \tag{32}$$

We note that in this case the friction coefficient is directly proportional to the eddy viscosity.

5. The mean flow

Utilizing (21)–(25), it is trivial to calculate the right-hand side of (3). In this problem, we note that $\overline{\tilde{u}\tilde{v}} = 0$. Hence, we can write the radiation stress components S_1 and S_2 in the x and y directions, respectively, by

$$S_1 = \int_{-h}^0 \frac{\overline{p_d}}{\rho} dz + \frac{g}{2}\overline{\tilde{\eta}^2} + \int_{-h}^0 \overline{\tilde{u}\tilde{u}\,dz} \quad \text{and} \tag{33}$$

$$S_2 = \int_{-h}^0 \frac{\overline{p_d}}{\rho} dz + \frac{g}{2}\overline{\tilde{\eta}^2} + \int_{-h}^0 \overline{\tilde{v}\tilde{v}\,dz}. \tag{34}$$

Utilizing that here $\overline{\tilde{u}\tilde{u}} = \overline{\tilde{v}\tilde{v}}\cos^2\beta$, we can write S_1 as

$$S_1 = S_2 - \sin^2\beta\int_{-h}^0 \overline{\tilde{v}\tilde{v}}\,dz. \tag{35}$$

Defining an integrated pressure $\overline{P}$ such that $\partial\overline{P}/\partial x = [\overline{p}_d(-h)\tan\beta]/\rho$, the total wave-forcing stress component S in the x direction in (4) becomes

$$S = S_1 - \overline{P} = S_2 - \sin^2\beta\int_{-h}^0 \overline{\tilde{v}\tilde{v}}\,dz - \overline{P}, \tag{36}$$

(see, e.g., Mei 1973). Utilizing (21)–(25), we find that the last two terms cancel exactly. Accordingly, we can write $S = S_2$, where

$$S = \frac{1}{4k\omega^2\sin\beta}\left(\frac{gk\eta_0}{1 - \Omega\cos\beta}\right)^2 \{2kx(\cos\beta - \Omega)\sin^2\beta$$
$$+ (\sin^2\beta + \Omega\cos\beta)(1 - \Omega\cos\beta) - [\Omega(1 - \Omega\cos\beta)\cos\beta]$$
$$\times\exp(-2b_r x\tan\beta)\}\exp(-2\alpha y - 2a_r x). \tag{37}$$

Hence, we find that the radiation stress component in the y direction also forces the flow in the x direction. In (37), a_r and b_r are given by (A10) and (A19), respectively. In these calculations, we have neglected all terms proportional to $(\alpha/k)^2$ and higher orders. We note that for $\Omega = 0$, (37) reduces to

$$S = \left(\frac{g^2 k\eta_0^2\sin\beta}{4\omega^2}\right)(2kx\cos\beta + 1)\exp(-2\alpha y - 2kx\cos\beta),$$

which is obtained from (12) and (13) of Weber and Ghaffari (2009).

The x and y components of the Lagrangian fluxes to the second order in wave steepness then become

$$\frac{\partial\overline{U}}{\partial t} - f\overline{V} + gh\frac{\partial\overline{\eta}}{\partial x} = -\frac{\partial S}{\partial x} - \tau_1 \quad \text{and}$$

$$\frac{\partial\overline{V}}{\partial t} + f\overline{U} + gh\frac{\partial\overline{\eta}}{\partial y} = -\frac{\partial S}{\partial y} - \tau_2. \tag{38}$$

It was demonstrated by Longuet-Higgins and Stewart (1960) that the radiation stress forcing would be $1/2(-\partial E/\partial y)$ for deep-water waves and $3/2(-\partial E/\partial y)$ for shallow-water waves in a nonrotating ocean of constant depth. As pointed out by Weber and Støylen (2011), the relation between the radiation stress components and the total wave energy depends on the wave type. For

example, for Poincaré waves in a shallow rotating ocean there is a velocity component in the cross-wave direction that contributes to the wave energy, but not to the radiation stress. Then, in this case $S_2 = 1/2(3 - f^2/\omega^2)E/\rho$. Because $|\omega| > |f|$ for Poincaré waves, we have that $S_2 < 3E/(2\rho)$ for this particular shallow-water problem. For the Stokes edge wave we also have a cross-wave velocity component, because the particles move in planes parallel to the sloping bottom. We therefore would expect a relation that differs from that of Longuet-Higgins and Stewart. In addition, the wave amplitude here decays exponentially in the cross-shore direction. It is therefore natural to consider the wave energy in the entire trapped region [i.e., (26)]. From (26) and (37) it is easy to see that

$$\langle S \rangle = E/\rho, \tag{39}$$

where $\langle S \rangle = \int_0^\infty S \, dx$. This is exactly the same result obtained by Weber and Ghaffari (2009) for the nonrotating Stokes edge wave, demonstrating that it is not the rotation but the sloping bottom that yields a value that is in between the deep- and shallow-water values of Longuet-Higgins and Stewart (1960).

Following Longuet-Higgins (1953), the Stokes drift to second order in wave steepness for this problem is easily obtained from the linear wave solutions (23)–(25).

By definition

$$\begin{aligned} \overline{v}_S &= \overline{\left(\int \tilde{u} \, dt \right) \tilde{v}_x} + \overline{\left(\int \tilde{v} \, dt \right) \tilde{v}_y} + \overline{\left(\int \tilde{w} \, dt \right) \tilde{v}_z} \\ &= \frac{\omega k \eta_0^2}{\sin^2\beta} \exp(-2a_r x + 2b_r z - 2\alpha y). \end{aligned} \tag{40}$$

We note that the Stokes drift has a maximum at the shoreline. Here,

$$\overline{v}_S(x = 0, z = 0) = \frac{\omega k \eta_0^2}{\sin^2\beta} \exp(-2\alpha y). \tag{41}$$

The alongshore Stokes flux for this problem becomes

$$\begin{aligned} \overline{V}_S &= \int_{-h}^0 \left[\overline{\left(\int \tilde{u} \, dt \right) \tilde{v}_x} + \overline{\left(\int \tilde{v} \, dt \right) \tilde{v}_y} + \overline{\left(\int \tilde{w} \, dt \right) \tilde{v}_z} \right] dz \\ &= \frac{1}{2\omega(1 - \Omega\cos\beta)\sin\beta} \left(\frac{gk\eta_0}{\omega} \right)^2 \\ &\quad \times [1 - \exp(-2b_r x \tan\beta)] \exp(-2a_r x - 2\alpha y). \end{aligned} \tag{42}$$

In the vertical wall limit ($\beta = \pi/2$), we must treat this problem with some care. Now, from (A15), (A10), and

(A19), we find $\omega^2 = gk$, $a_r = -fk/\omega$, and $b_r = k$. The Stokes drift (40) then becomes

$$\overline{v}_S(\beta = \pi/2) = \omega k \eta_0^2 \exp\left(\frac{2fk}{\omega} x + 2kz - 2\alpha y \right). \tag{43}$$

We note that trapping now requires $\omega < 0$. The resulting wave motion is a coastal Kelvin wave propagating with the coast (the vertical wall) to the right in the Northern Hemisphere. The trapping distance is the baroclinic Rossby radius $(|\omega|/k)/f$. In this limit the Stokes flux must be obtained from (43) by integrating in the vertical from minus infinity to zero, yielding

$$\overline{V}_S(\beta = \pi/2) = \frac{1}{2} \omega \eta_0^2 \exp\left(\frac{2kf}{\omega} x - 2\alpha y \right). \tag{44}$$

For slope angles in the interval $0 < \beta < \pi/2$, we can apply (42) and expand the exponential functions for small x. We then obtain

$$\overline{V}_S = \frac{k\omega\eta_0^2}{\sin\beta \cos\beta} x \exp(-2\alpha y). \tag{45}$$

In this paper, we shall work with depth-averaged drift velocities. We define the depth-averaged Stokes drift by

$$\hat{v}_S = \frac{\overline{V}_S}{h}, \tag{46}$$

where $h = x \tan\beta$, and $\overline{V}_S$ is given by (42). By comparison with (41), we note from (45) and (46) that $\hat{v}_S$ yields the correct Stokes drift at the shoreline, that is,

$$\hat{v}_S(x = 0) = \overline{v}_S(x = 0, z = 0) = v_{S0} \exp(-2\alpha y), \tag{47}$$

where

$$v_{S0} = \frac{k\omega\eta_0^2}{\sin^2\beta}. \tag{48}$$

The Stokes drift is basically related to the net particle motion in inviscid waves, and there is no Stokes drift in the direction perpendicular to the wave propagation direction. In the presence of friction in the fluid, the Longuet-Higgins formulation yields a small drift in the cross-wave direction, being proportional to the small friction coefficient. This part is inseparable from the frictional mean Eulerian current in the cross-wave direction, into which it can be included (see, e.g., Weber and Drivdal 2012). Hence, we take that the Stokes flux in the x direction $\overline{U}_S$ is zero. Thus, the total wave momentum in the trapped region becomes, from (42),

$$M_w = \rho \int_0^\infty \overline{V}_S \, dx = \frac{\rho g \eta_0^2}{4\omega(\cos\beta - \Omega)} \exp(-2\alpha y). \qquad (49)$$

We note that for $\beta = \pi/2$, the total wave momentum could equally well have been obtained by integrating (44) for the vertical wall limit. By comparing with the total energy density (26), we note that for this problem $E = M_w c^*$, where $c^* = (2 - \Omega\cos\beta)\omega/(2k)$. In a non-rotating ocean where $f = 0$, c^* becomes equal to the phase speed $c = \omega/k$, so then $E = M_w c$ (see, e.g., Starr 1959).

When we express the solutions as expansions in power series after the wave steepness as a small parameter, which is the basis of the derivation of the flux equations of (4), we must require that the second-order Stokes velocity must be considerably smaller than the linear velocity field, which in turn must be smaller than the phase speed of the wave. From (24) and (48), utilizing (A16), the conditions $|\hat{v}_S| \ll |\tilde{v}|$ and $|\tilde{v}| \ll |\omega|/k$ both lead to

$$k\eta_0 \ll \sin\beta. \qquad (50)$$

This condition must be fulfilled for the Stokes edge wave when applying the nonlinear theory for calculating wave-induced mean drift currents in practical cases.

6. The steady Eulerian mass transport

As first shown by Longuet-Higgins (1953), the mean wave-induced Lagrangian velocity could be written as a sum of the Stokes drift and a mean Eulerian current, where the latter depended on friction. Hence, the mean Eulerian volume fluxes in this problem can be written

$$\overline{U}_E = \overline{U}_L \quad \text{and}$$
$$\overline{V}_E = \overline{V}_L - \overline{V}_S, \qquad (51)$$

where the Lagrangian fluxes $(\overline{U}_L, \overline{V}_L)$ are equal to $(\overline{U}, \overline{V})$ in (38), and $(\overline{V}_S)$ is given by (40).

For a given wave field (and Stokes drift) at $t = 0$, as assumed in this paper, the solutions for $\overline{U}_E$ and $\overline{V}_E$ will contain a transient part. For a complete solution we must state the appropriate initial conditions for this flow, which we really do not know. But as time moves on, the solution will equilibrate toward a steady state, independent of the initial conditions. We here focus on this asymptotic solution for large t. The steady-state governing momentum of (38) then reduces to

$$-f\overline{V}_E + gh\frac{\partial\overline{\eta}}{\partial x} = f\overline{V}_S - \frac{\partial S}{\partial x} - \tau_1 \quad \text{and}$$
$$f\overline{U}_E + gh\frac{\partial\overline{\eta}}{\partial y} = -\frac{\partial S}{\partial y} - \tau_2. \qquad (52)$$

In the steady case, utilizing (51), the integrated continuity equation in (4) becomes

$$\frac{\partial\overline{U}_E}{\partial x} + \frac{\partial\overline{V}_E}{\partial y} = -\frac{\partial\overline{V}_S}{\partial y}. \qquad (53)$$

At the coast, we must have

$$\overline{U}_E\big|_{x=0} = 0. \qquad (54)$$

We consider mean flow trapped over the slope. Then, we must require

$$\overline{V}_E \to 0 \quad \text{and} \quad x \to \infty. \qquad (55)$$

The mean motion in the cross-shore direction is small, and we neglect the effect of friction in this direction. Then, from the curl of (52)

$$g\overline{\eta}_y \tan\beta = -\tau_{2x}. \qquad (56)$$

Assuming that $\overline{\eta} \propto \exp(-2\alpha y)$, we find that

$$gh\overline{\eta}_x = \frac{1}{2\alpha}x\tau_{2xx}. \qquad (57)$$

Then by inserting into the cross-shore component of (52), we find

$$x\tau_{2xx} - 2\alpha f\overline{V}_E = 2\alpha(f\overline{V}_S - S_x). \qquad (58)$$

In a vertically integrated approach, the friction term in (58) must be modeled. Often one uses a formulation where the bottom stress is proportional to the square of the mean velocity in the problem. A similar effect is obtained by defining a friction coefficient that is proportional to the bottom drag coefficient times a characteristic velocity (see, e.g., Nøst 1994). Then the bottom friction becomes linear in the mean velocity, which simplifies the analysis. We use this approach here and take

$$\tau_2 = K\hat{v}_E, \qquad (59)$$

where $\hat{v}_E = \overline{V}_E/h$ is the vertically averaged Eulerian velocity, and K is a constant friction coefficient (dimension velocity). The present approach separates the decay of wave momentum from the frictional influence on the mean flow as suggested in the literature (Jenkins 1989; Weber and Melsom 1993; Ardhuin and Jenkins 2006). Using (59), and introducing the vertically averaged velocities, we find from (58) when $x \neq 0$,

$$\hat{v}_{Exx} - \frac{2\alpha\tan\beta}{K}\hat{v}_E = \frac{2\alpha}{K}\left[(f\tan\beta)\hat{v}_S - \frac{1}{x}S_x\right]. \quad (60)$$

Applying (54), the y component of (52) at the coast reduces to

$$\tau_2 = 2\alpha S \quad \text{at} \quad x = 0. \quad (61)$$

Then, utilizing (37) and (59), (61) yields the boundary condition

$$\hat{v}_E = v_{E0}\exp(-2\alpha y) \quad \text{at} \quad x = 0, \quad (62)$$

where

$$v_{E0} = \frac{\alpha g\eta_0^2}{2K}. \quad (63)$$

Using (31), we find

$$v_{E0} = \frac{\nu k}{K}\left(\frac{k\omega\eta_0^2}{\sin\beta}\right)\left[1 + \frac{1}{2}\left(\frac{f\omega}{gk}\right)^2\right]. \quad (64)$$

Furthermore, for trapped mean motion, we must require

$$\hat{v}_E \to 0 \quad \text{when} \quad x \to \infty. \quad (65)$$

In (64) the ratio $\nu k/K$ expresses the balance between the forcing from the wave field (through the radiation stress) and the bottom stress on the mean flow. This ratio may vary numerically for various wave conditions, but from a physical balance point of view, its magnitude should be of the order of unity.

We now introduce a nondimensional alongshore Eulerian drift velocity $Q_E(x)$ by

$$Q_E = \frac{\hat{v}_E}{v_{E0}\exp(-2\alpha y)}. \quad (66)$$

We also define a nondimensional cross-shore coordinate $X = 2a_r x$. The governing (60) then becomes

$$Q_E'' - \gamma^2 Q_E = \exp(-X) + \frac{1}{X}[F_1\exp(-X) + F_2(-\sigma X)], \quad (67)$$

where the primes denote differentiation with respect to X. The boundary conditions are

$$Q_E = 1, \quad X = 0, \quad \text{and}$$
$$Q_E \to 0, \quad X \to \infty. \quad (68)$$

In (67), we have defined the nondimensional parameters γ and σ as

$$\gamma^2 = \frac{\alpha f\tan\beta}{2Kk^2}\left(\frac{1 - \Omega\cos\beta}{\cos\beta - \Omega}\right)^2 \quad (69)$$

and

$$\sigma = \frac{1 - \Omega\cos\beta}{(\cos\beta - \Omega)\cos\beta}. \quad (70)$$

Utilizing (37) and (40), we find that the coefficients in (67) can be written

$$F_1 = \frac{\Omega(1 - 2\Omega\cos\beta + \cos^2\beta)}{(\cos\beta - \Omega)\sin^2\beta} \quad \text{and}$$
$$F_2 = -\frac{2\Omega(1 - \Omega\cos\beta)}{(\cos\beta - \Omega)\sin^2\beta}. \quad (71)$$

Before attempting to solve (67), we observe the following: to have solutions that are trapped over the slope in a rotating ocean ($f > 0$), we must require that the complementary part of the solution has an exponential behavior (i.e., that $\gamma^2 > 0$). For $\omega > 0$, $\alpha > 0$, and β in the range $0 < \beta < \beta^*$, that is, waves propagating with the coast to the left in the Northern Hemisphere, this is fine. But for waves propagating with the coast to the right, we have $\omega < 0$, $\alpha < 0$, and hence $\gamma^2 < 0$. This yields a sinusoidal complementary part with no seaward limitation. Hence, for the damped Stokes edge wave that propagates with the coast to the right, the induced Stokes drift is trapped over the slope (because the primary wave field is trapped), but the frictionally induced mean Eulerian current is not. Accordingly, there is no steady trapped solution to the Eulerian drift problem induced by such waves. Any transient behavior will not be pursued here. When the effect of the earth's rotation can be neglected ($f = 0$), then $\gamma = 0$, and we have trapping of the Eulerian flow also when $\omega < 0$. The details concerning the solution of (67) have been deferred to appendix B.

We introduce the nondimensional average Stokes drift velocity Q_S from (46) and (63) by

$$Q_S = \frac{\hat{v}_S}{v_{E0}\exp(-2\alpha y)}$$
$$= \frac{2Kk^2(\cos\beta - \Omega)\cos\beta}{\alpha\omega(1 - \Omega\cos\beta)\sin^3\beta}\frac{1}{X}[\exp(-X) - \exp(-\sigma X)]. \quad (72)$$

The expression for Q_E is given by (B10). The vertically averaged nondimensional Lagrangian drift velocity Q_L thus becomes

$$Q_L = Q_E + Q_S. \quad (73)$$

7. Results

a. General discussion

To quantify the derived wave-induced mean currents, we must assess the values of the physical parameters in this problem. For the modeling of tidal currents in the Barents Sea, a typical value of the eddy viscosity is $\nu = 10^{-3}\,\mathrm{m^2\,s^{-1}}$ (Nøst 1994). At a sloping beach, eddy viscosity estimates are higher by a factor of 10–$50\,\mathrm{m^2\,s^{-1}}$ (Apotsos et al. 2007), mainly due to turbulence induced by breaking waves. Without specifying the source of turbulence, which is outside the scope of this paper, it seems reasonable to take ν from 1×10^{-2} to $5 \times 10^{-2}\,\mathrm{m^2\,s^{-1}}$ in quantifying the drift induced by trapped waves (see Mei et al. 1998). By specifying the eddy viscosity ν that acts to dampen the linear wave field, we obtain the friction coefficient r and the spatial wave attenuation coefficient α from (32) and (A21) for prescribed wavelength and bottom slope. As explained in the previous section, the relation between the linear friction coefficient K and the bottom drag coefficient c_B for the mean flow can be approximated as $K = c_B v_B$, where v_B is a typical near-bottom mean velocity (Gjevik et al. 1994; Nøst 1994).

The bottom drag coefficient depends on the seabed conditions, for example, the presence of ripples (Longuet-Higgins 2005). Very close to the bottom in shallow waters, the mean horizontal stresses are partly used to accelerate sediment particles that are kept in suspension by the oscillating wave motion. This part of the stress is not felt by the water column just above the rippled bed. The effect of the sediment transport must be reflected in the value of the bottom drag coefficient. For a corrugated bed, $c_B = 0.1$ appears to be an appropriate value for short waves (Longuet-Higgins 2005). For longer waves and deeper waters, c_B will be considerably smaller, typically $c_B = \sim 10^{-3}$ (see Gjevik et al. 1994; Nøst 1994). Taking $v_B = \sim 10^{-2}\,\mathrm{m\,s^{-1}}$, we obtain that $K = \sim 10^{-3}\,\mathrm{m\,s^{-1}}$ and $K \sim 10^{-5}\,\mathrm{m\,s^{-1}}$ in the short- and long-wave limit, respectively.

In discussing the general properties of the solutions, we take that the wavelength $\lambda = 2\pi/k$ is 1 km and use $f = 1.2 \times 10^{-4}\,\mathrm{s^{-1}}$. For waves traveling with the coast to the left ($\omega > 0$), the critical slope angle (A18) becomes $\beta^* \approx 89.9°$, which is very close to the vertical wall limit. Hence, in practice, the admissible slopes in this example belong to the interval $0 < \beta < \pi/2$. In this case $\Omega = f/\omega = 3.7 \times 10^{-3}$, so the effect of the earth's rotation can be neglected. Then in the solution (72) for the Stokes drift $\sigma = 1/\cos^2\beta > 1$. Furthermore, in this example we have taken $\nu = 1 \times 10^{-2}\,\mathrm{m^2\,s^{-1}}$ and $K = 10^{-5}\,\mathrm{m\,s^{-1}}$, according to the discussion above.

In Fig. 2, we have displayed Q_E from (B10) for various values of the bottom slope ($\beta = 1°, 30°, 45°$, and $85°$). We

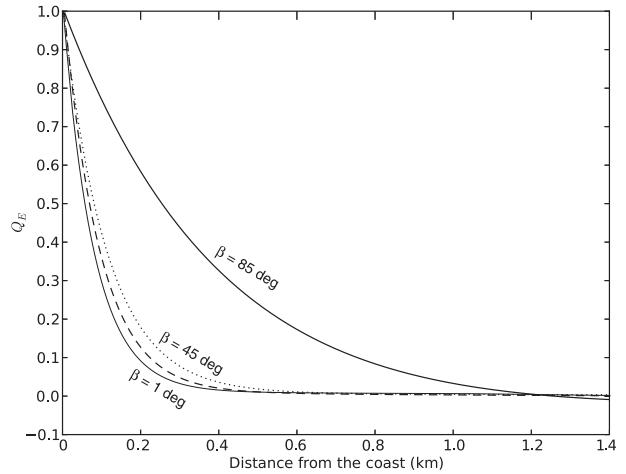

FIG. 2. Nondimensional mean Eulerian current for $\lambda = 1$ km and $\beta = 1°$ (thin solid line), $\beta = 30°$ (dashed line), $\beta = 45°$ (dotted line), and $\beta = 85°$ (thick solid line) as a function of the seaward coordinate.

note from the figure that larger slope angles mean a wider trapping region. If we compare with the Stokes drift in (72), which varies over the shelf as $[\exp(-X) - \exp(-\sigma X)]/(\sigma - 1)$, where X is nondimensional, we find that this is very close to the variation of Q_E in Fig. 2 for small and moderate angles.

Although the spatial variation over the shelf for Q_E and Q_S is not very different for small and moderate slopes, this is not so for the maximum current values at the shoreline, which depend very much on the slope angle. In fact, by forming the ratio between the mean Eulerian current and the Stokes drift at the shore, we find from (48) and (64) that

$$d = \frac{v_{E0}}{v_{S0}} = \frac{\nu k}{K} \sin\beta \left[1 + \frac{1}{2}\left(\frac{f\omega}{gk}\right)^2 \right]. \quad (74)$$

We note immediately that increasing values of f act to favor v_{E0}. However, for the wavelengths considered here, the last term in the parentheses is negligible. Then, the relative strength between v_{E0} and v_{S0} depends on friction and wave slope. We have argued before that for the frictional influence, there should be a balance so $\nu k/K$ should be of the order of unity. In the present example this ratio is 6.3. Hence, in (74) the slope angle is the crucial parameter. In Fig. 3, we have plotted the nondimensional currents Q_E and Q_S for various values of the slope angle. As noted from Fig. 2, the spatial variation of Q_S is nearly the same for small and moderate slopes. In the figure we have chosen Q_E ($\beta = 2.8°$). We see from Fig. 3 that for small angles the Stokes drift dominates in this example. The currents are comparable
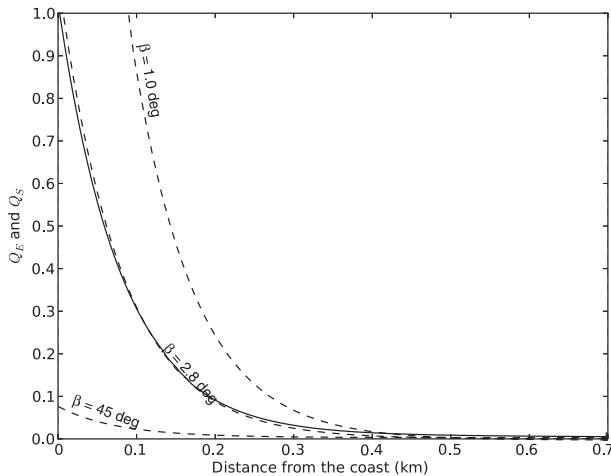
FIG. 3. Nondimensional Eulerian mean current Q_E for $\beta = 2.8°$ (solid line) and nondimensional Stokes drift current Q_S (broken line) as a functions of the seaward coordinate. Here $\lambda = 1$ km, and β varies from $1°$ to $45°$.

in magnitude to $\beta = 2.8°$. We have considered $\beta = 1°$ as the lower limit. This is the slope used by Kenyon (1969) in his calculations of the Stokes drift.

In reality, bottom slopes are not very steep. In fact, in the practical examples we consider at the end of this section, they are less than $10°$. However, our calculations for $\omega > 0$ are valid for all $\beta < \beta*$ [see (A18)]. Such solutions may be convenient for comparison with experiments in wave tanks, where for laboratory model purposes a steep slope may be advantageous.

In practice, there is a limitation to the wavenumber in this problem. The theory of the Stokes edge wave requires a constant bottom slope, but in real cases the (approximately linear) bottom profile may change quite abruptly at a distance L from the shoreline. To have trapped waves within the constant slope region, we then must require

$$a_r L > 1 \qquad (75)$$

where a_r is given by (A10). For not too long waves, and normal small slope angles, we can use the nonrotating limit. Then, (75) reduces to

$$k > L^{-1}. \qquad (76)$$

b. Specific case studies

The existence of edge waves on natural shorelines has been inferred from the periodic spacing of rip currents (Bowen and Inman 1969) and forming of beach cusps and crescentic bars (Bowen and Inman 1971). The theory developed here is valid for slope angles in the

interval $0 < \beta \leq \pi/2$. However, in natural environments most beach slopes are quite gentle. To relate our theoretical results to the natural environment, we consider two different locations where we find short and long waves, respectively: first, Slapton Beach (Huntley and Bowen 1973) and second, Lake Michigan (Donn and Ewing 1956). In both cases, the depth increases slowly from the coast. As noted before, in such cases the Stokes drift is comparable to or exceeds the mean Eulerian current.

For short waves, we used the field observation at Slapton Beach by Huntley and Bowen (1973). They demonstrated that the observed wave field at 0.1 Hz did represent a Stokes standing edge wave. For such high-frequency waves, the effect of the earth's rotation can safely be neglected. The field survey yielded a wavelength of about 30 m. The beach profile in the intertidal zone could be approximated by the expression $h = h_0[1 - \exp(-ax)]$, where $h_0 = 7.05$ m and $a = 0.03$ m^{-1}. Because the trapping distance in this case is about 30 m from the shoreline, we take the equivalent linear slope angle to be $\beta = 10°$. Based on the observed along- and cross-shore velocities, we estimate a wave amplitude of 0.2 m for the standing edge wave. It seems reasonable to use half the standing wave amplitude for our progressive wave; that is, we take $\eta_0 = 0.1$ m in our calculations. With these parameters the Stokes drift at coast becomes $v_{S0} = 4.4$ cm s^{-1}. We use the eddy viscosity and bottom drag coefficient values for short waves ($\nu = 3 \times 10^{-2}$ m^2 s^{-1} and $K = 10^{-3}$ m s^{-1}). From (63), we find $v_{E0} = 4.8$ cm s^{-1}, which is comparable to the Stokes drift. Here $\nu k/K = 6.3$. In this example, $k\eta_0 = 0.02$ and $\sin\beta = 0.17$, which fulfils (50) quite well.

Our second example is from Lake Michigan. The disastrous surge in 1954 and the resulting gravity waves were explained by Ewing et al. (1954) as a resonant coupling between a fast-moving atmospheric squall line and the Stokes edge wave. They utilized the theory of edge waves (Stokes 1846; Ursell 1951, 1952) in order to explain the long-period high waves (periods of the order of 100 min) that were correlated with atmospheric pressure jumps (Donn and Ewing 1956). In Lake Michigan, the Stokes edge wave propagated with the coast to the right ($\omega < 0$), so formally the wave-induced Eulerian current is not trapped to the coast in the presence of rotation. However, the effect of rotation is negligible for edge waves with periods of the order of 100 min in this body of water ($f\omega/gk = 2.7 \times 10^{-3} \ll 1$). In Lake Michigan, storm surge data from Waukegan yields a typical wave period of 109 min and a wave amplitude of about 3 m. A typical slope angle for Lake Michigan is $0.17°$, and $f = 1.01 \times 10^{-4}$ s. Then, with $\omega = -9.61 \times 10^{-4}$ s^{-1}, we find that $v_{S0} = -3.4$ cm s^{-1}. Using

$\nu = 3 \times 10^{-2}\,\mathrm{m^2\,s^{-1}}$ and $K = 10^{-5}\,\mathrm{m\,s^{-1}}$, we obtain v_{E0} $\sim 10^{-3}\,\mathrm{cm\,s^{-1}}$, so the Stokes drift dominates completely in this example. Despite the large amplitude, the Stokes drift is quite moderate. This is because the waves are quite long. With a period of 109 min, we find for the wavenumber in this problem that $k = 3.5 \times 10^{-5}\,\mathrm{m^{-1}}$, then $\lambda = \sim 180\,\mathrm{km}$. Finally, in this example $\eta_0 k = 1.1 \times 10^{-4}$, and $\sin\beta = 3.0 \times 10^{-3}$ that fulfils (50) very well.

8. Discussion and concluding remarks

In a previous paper (Weber and Ghaffari 2009), we investigated the nonlinear mass transport in the Stokes surface edge wave in an unbounded nonrotating ocean. This was done by applying an Eulerian description of motion and expanding the solution in series after wave steepness as a small parameter. Utilizing almost the same approach, we have derived an analytical expression for the vertically averaged Lagrangian drift velocity induced by the Stokes edge wave in a rotating ocean. This drift is composed of a Stokes drift component plus an Eulerian mean velocity, where the former is inherent in the wave motion and the latter arises from the effect of friction. Similar to the nonrotating case, the time rate of change of the total Lagrangian momentum flux in the wave direction (y direction) is forced by the divergence of the total energy density $-\partial E/\partial y$, which is midway between the deep- and shallow-water values for the nonrotating surface waves in an ocean of constant depth (Longuet-Higgins and Stewart 1960). The main aim of this paper has been to quantify the contributions of the Stokes and Eulerian mean currents to the vertically averaged mean Lagrangian drift velocity.

The calculations show that the Stokes drift and the Eulerian current attain their maximum values at the shoreline. For wave motion in which the earth's rotation becomes important, we find that this effect tends to enhance the mean Eulerian current for the given bottom slope. When we can neglect the effect of the earth's rotation, the relative importance of the mean Eulerian current to the Stokes drift can be expressed as $v_{E0}/v_{S0} = \nu k \sin\beta/K$, demonstrating that, for the given wavelength, the Stokes drift tends to dominate for small bottom slopes. This is a novel result and shows that for most natural beach or coastal situations it is sufficient to calculate the Stokes drift in the Stokes edge wave in order to obtain the main part of the Lagrangian alongshore drift velocity.

The transfer of mean momentum from damped waves to mean Eulerian currents follows from the fundamental concept of conservation of total momentum. To balance the Eulerian flow, friction is needed. In the present paper, we use a simple linear model for the bottom friction that does this task. Because ocean flows are turbulent, we have to use eddy values for the friction coefficients. Although these coefficients are assessed from physical reasoning, their values can never be established with absolute certainty. Despite those objections, it is of fundamental importance to include the wave-induced mean Eulerian current as a part of the total drift current. However, natural beach or coastal slopes are rather gentle. As demonstrated in the present paper for the Stokes edge wave, this tends to enhance the Stokes drift relative to the mean Eulerian current in their contribution to the mean Lagrangian drift velocity. The Stokes drift follows basically from inviscid wave theory and is easy to calculate. For steeper slopes, the importance of the Eulerian current increases, as noted from our example from Slapton Beach. Because steep slopes are easily made in the laboratory, our analytical results for a large bottom slope may be of importance for comparisons with (future) laboratory experiments in rotating tanks. In conclusion, we find that the Stokes edge wave induces a mean drift velocity that may be of importance for the alongshore transport of pollutants, biological materials, and suspended loads.

APPENDIX A

Determination of Parameters

Inserting from (10) and (11) into the boundary condition (16), we obtain

$$\omega^2 + i\omega r - gb = 0. \qquad (A1)$$

To the lowest order in the small quantities, we obtain from the real and imaginary parts

$$\omega^2 = gb_r \quad \text{and} \qquad (A2)$$

$$b_i = \frac{\omega r}{g} = Rb_r. \qquad (A3)$$

By inserting (12) into (9), utilizing (A3), we obtain from the real and imaginary parts, respectively,

$$(1 - \Omega^2)b_r^2 + a_r^2 - k^2 = 0 \quad \text{and} \qquad (A4)$$

$$-k\alpha + a_r a_i + Rb_r^2 = 0. \qquad (A5)$$

Inserting (13) and (15) into the boundary condition (17), again utilizing (A3), we obtain

$$(1 - \Omega^2)b_r - (\Omega k + a_r)\tan\beta = 0 \quad \text{and} \quad \text{(A6)}$$

$$(1 - \Omega^2)(\Omega\alpha + a_i + Ra_r) - 2R(\Omega k + a_r) = 0. \quad \text{(A7)}$$

From (A4) and (A6), we find expressions for a_r and b_r. In particular

$$a_r = \frac{k}{1 - \Omega^2\cos^2\beta}[-\Omega + \Omega\cos^2\beta \pm (1 - \Omega^2)\cos\beta].$$
$$\text{(A8)}$$

For two signs in (84), we apply the identities

$$-\Omega + \Omega\cos^2\beta + \cos\beta - \Omega^2\cos\beta$$
$$= (\cos\beta - \Omega)(\Omega\cos\beta + 1) \quad \text{and}$$

$$-\Omega + \Omega\cos^2\beta - \cos\beta + \Omega^2\cos\beta$$
$$= -(\cos\beta + \Omega)(\Omega\cos\beta - 1). \quad \text{(A9)}$$

Hence, for the plus and minus signs, respectively

$$a_{r+} = \frac{k(\cos\beta - \Omega)}{1 - \Omega\cos\beta} \quad \text{and} \quad \text{(A10)}$$

$$a_{r-} = -\frac{k(\Omega + \cos\beta)}{1 + \Omega\cos\beta}. \quad \text{(A11)}$$

In this study we take that $f > 0$ (Northern Hemisphere), so the sign of $\Omega = f/\omega$ depends solely on ω. As noted in connection with (10), trapping at the coast requires $a_r > 0$. To have trapped waves that travel in both directions along the coast ($\Omega > 0$, $\Omega < 0$), we must exclude the a_{r-} solution. This is shown as follows: from (A2) and (A6) we have a general expression for a_r:

$$a_r = \frac{(1 - \Omega^2)\omega^2}{g\tan\beta} - k\Omega. \quad \text{(A12)}$$

By taking $a_{r-} = a_r$ we readily obtain

$$\omega^2 + (f\cos\beta)\omega + gk\sin\beta = 0. \quad \text{(A13)}$$

Hence

$$1 + \Omega\cos\beta = -\frac{gk\sin\beta}{\omega^2} < 0. \quad \text{(A14)}$$

Obviously, this cannot be true for $\Omega > 0$. For $\Omega < 0$, (A14) requires $\Omega < -1/\cos\beta$. But in this case, we note from (A11) that $a_{r-} < 0$. Hence, a_{r-} must be discarded

for $\Omega > 0$ as well as for $\Omega < 0$. For $a_{r+} = a_r$ in (A12), we obtain

$$\omega^2 - (f\cos\beta)\omega - gk\sin\beta = 0. \quad \text{(A15)}$$

Now

$$1 - \Omega\cos\beta = \frac{gk\sin\beta}{\omega^2} > 0. \quad \text{(A16)}$$

In this case, we note that $a_{r+} > 0$ for all $\omega < 0$ (waves with the coast to the right). For waves with the coast to the left ($\omega > 0$), we see from (A10) that trapping requires $\cos\beta > \Omega$ (Johns 1965). The correct dispersion relation for this problem is (A15), leading to the two roots (Weber 2012)

$$\omega_1 = \frac{1}{2}f\cos\beta + \frac{1}{2}(f^2\cos^2\beta + 4gk\sin\beta)^{1/2} > 0 \quad \text{and}$$

$$\omega_2 = \frac{1}{2}f\cos\beta - \frac{1}{2}(f^2\cos^2\beta + 4gk\sin\beta)^{1/2} < 0.$$
$$\text{(A17)}$$

Here ω_1 is the frequency of a trapped wave that travels with the coast to the left, while ω_2 represents a wave traveling with the coast to the right in the Northern Hemisphere. The limiting, trapping angle β^* for ω_1 is given in Weber (2012). Inserting $\cos\beta^* = f/\omega_1(\beta^*)$ into (A15) yields

$$\beta^* = \arcsin[(\delta^2 + 1)^{1/2} - \delta], \quad \text{(A18)}$$

where $\delta = f^2/(2gk)$. For $\beta > \beta^*$, there exists no trapped wave traveling with the coast to the left. With $a_r = a_{r+}$, we obtain from (A6)

$$b_r = \frac{k\sin\beta}{1 - \Omega\cos\beta}. \quad \text{(A19)}$$

Then, from (A3), we obtain

$$b_i = \frac{Rk\sin\beta}{1 - \Omega\cos\beta}. \quad \text{(A20)}$$

By combining (A5) and (A7), we obtain for the damping rate

$$\alpha = \frac{Rk}{1 - \Omega\cos\beta}. \quad \text{(A21)}$$

Because $1 - \Omega_{1,2}\cos\beta > 0$, see (A16), we note that $\alpha > 0$ for $\omega = \omega_1 > 0$, and $\alpha < 0$ for $\omega = \omega_2 < 0$. In the latter case the propagation is in the negative y direction, and we consider damped, trapped waves in the interval $-\infty < y \leq 0$, that is, $\exp(-\alpha y) \leq 1$ in (21)–(25). Finally, by inserting into (A5), we obtain

$$a_i = \frac{Rk \cos\beta}{1 - \Omega \cos\beta}. \qquad (A22)$$

APPENDIX B

Analytical Solution for the Mean Eulerian Flow

An analytical solution of (67) can be found in terms of exponential integrals (see, e.g., Weber and Støylen 2011). Assuming that γ^2 is a positive constant, the complementary part $Q_E^{(c)}$ of the solution becomes

$$Q_E^{(c)} = C_1 \exp(\gamma X) + C_2 \exp(-\gamma X), \qquad (B1)$$

where C_1 and C_2 are constants. Applying the variation of the parameters method, we write the particular solution $Q_E^{(p)}$ as

$$Q_E^{(p)} = m_1(X) \exp(\gamma X) + m_2(X) \exp(-\gamma X). \quad (B2)$$

The functions m_1 and m_2 are then determined by

$$m_1' \exp(\gamma X) + m_2' \exp(-\gamma X) = 0 \quad \text{and}$$

$$\gamma m_1' \exp(\gamma X) - \gamma m_2' \exp(-\gamma X) = G(X), \qquad (B3)$$

where primes denote derivation with respect to X, and

$$G(X) = \exp(-X) + \frac{1}{X}[F_1 \exp(-X) + F_2 \exp(-\sigma X)]. \qquad (B4)$$

The Wronskian in this problem is -2γ. Hence, we find

$$m_1 = \frac{1}{2\gamma} \int \exp(-\gamma X) G(X)\, dX \quad \text{and}$$

$$m_2 = -\frac{1}{2\gamma} \int \exp(\gamma X) G(X)\, dX. \qquad (B5)$$

We can express the terms with a singularity at $X = 0$ as exponential integrals E_i (e.g., Abramowitz and Stegun 1972). By definition

$$E_i(X) = \int_{-\infty}^{X} \frac{\exp(t)}{t}\, dt. \qquad (B6)$$

Hence, (B2) can be written

$$Q_E^{(p)} = -\frac{1}{\gamma^2 - 1} \exp(-X) + \frac{F_1}{2\gamma} \{\exp(\gamma X) E_i[-(\gamma + 1)X] - \exp(-\gamma X) E_i[(\gamma - 1)X]\}$$

$$+ \frac{F_2}{2\gamma} \{\exp(\gamma X) E_i[-(\gamma + \sigma)X] - \exp(-\gamma X) E_i[(\gamma - \sigma)X]\}. \qquad (B7)$$

For the special case $\gamma = 1$, m_1 in (B5) becomes unaltered, while

$$m_2 = -\frac{1}{2} \{X + F_1 \ln X + F_2 E_i[(1 - \sigma)X]\}. \quad (B8)$$

To satisfy the boundary conditions (68), we must require for the complementary solution (B1) that

$$C_1 = 0 \quad \text{and}$$

$$C_2 = 1 - Q_E^{(p)}\big|_{x \to 0^+} \qquad (B9)$$

Inserting from (B7) and (B9), the complete solution for the nondimensional mean Eulerian drift velocity becomes

$$Q_E = C_2 \exp(-\gamma X) + Q_E^{(p)}. \qquad (B10)$$

REFERENCES

Abramowitz, M., and I. Stegun, Eds., 1972: *Handbook of Mathematical Functions, with Formulas, Graphs, and Mathematical Tables.* National Bureau of Standards Applied Mathematics Series, Vol. 55, United States Government Printing Office, 1046 pp.

Apotsos, A., B. Raubenheimer, S. Elgar, R. T. Guza, and J. A. Smith, 2007: Effects of wave rollers and bottom stress on wave setup. *J. Geophys. Res.,* **112,** C02003, doi:10.1029/2006JC003549.

Ardhuin, F., and A. D. Jenkins, 2006: On the interaction of surface waves and upper ocean turbulence. *J. Phys. Oceanogr.,* **36,** 551–557, doi:10.1175/JPO2862.1.

Bowen, A. J., and D. L. Inman, 1969: Rip currents: 2. Laboratory and field observations. *J. Geophys. Res.,* **74** (23), 5479–5490, doi:10.1029/JC074i023p05479.

——, and ——, 1971: Edge waves and crescentic bars. *J. Geophys. Res.,* **76** (36), 8662–8671, doi:10.1029/JC076i036p08662.

Donn, W. L., and M. Ewing, 1956: Stokes' edge waves in Lake Michigan. *Science,* **124,** 1238–1242, doi:10.1126/science.124.3234.1238.

Ewing, M., F. Press, and W. L. Donn, 1954: An explanation of the Lake Michigan wave of 26 June 1954. *Science,* **120,** 684–686, doi:10.1126/science.120.3122.684.

Gaster, M., 1962: A note on the relation between temporally-increasing and spatially-increasing disturbances in hydrodynamic stability. *J. Fluid Mech.,* **14,** 222–224, doi:10.1017/S0022112062001184.

Gjevik, B., E. Nøst, and T. Straume, 1994: Model simulations of the tides in the Barents Sea. *J. Geophys. Res.,* **99** (C2), 3337–3350, doi:10.1029/93JC02743.

Greenspan, H. P., 1970: A note on edge waves in a stratified fluid. *Stud. Appl. Math.,* **49,** 381–388.

Huntley, D. A., and A. J. Bowen, 1973: Field observations of edge waves. *Nature,* **243,** 160–162, doi:10.1038/243160a0.

Jenkins, A. D., 1989: The use of a wave prediction model for driving a near-surface current model. *Dtsch. Hydrogr. Z.,* **42,** 133–149, doi:10.1007/BF02226291.

Johns, B., 1965: Fundamental mode edge waves over a steeply sloping shelf. *J. Mar. Res.,* **23,** 200–206.

Kenyon, K. E., 1969: Note on Stokes' drift velocity for edge waves. *J. Geophys. Res.,* **74** (23), 5533–5535, doi:10.1029/JC074i023p05533.

LeBlond, P. H., and L. A. Mysak, 1978: *Waves in the Ocean.* Elsevier Oceanography Series, Vol. 20, Elsevier, 602 pp.

Llewellyn Smith, S. G., 2004: Stratified rotating edge waves. *J. Fluid Mech.,* **498,** 161–170, doi:10.1017/S002211200300702X.

Longuet-Higgins, M. S., 1953: Mass transport in water waves. *Philos. Trans. Roy. Soc. London,* **A245,** 535–581, doi:10.1098/rsta.1953.0006.

——, 2005: On wave set-up in shoaling water with a rough seabed. *J. Fluid Mech.,* **527,** 217–235, doi:10.1017/S0022112004003222.

——, and R. W. Stewart, 1960: Changes in the form of short gravity waves on long waves and tidal currents. *J. Fluid Mech.,* **8,** 565–583, doi:10.1017/S0022112060000803.

Mei, C. C., 1973: A note on the averaged momentum balance in two-dimensional water waves. *J. Mar. Res.,* **31,** 97–104.

——, C. Chian, and F. Ye, 1998: Transport and resuspension of fine particles in a tidal boundary layer near a small peninsula. *J. Phys. Oceanogr.,* **28,** 2313–2331, doi:10.1175/1520-0485(1998)028<2313:TAROFP>2.0.CO;2.

Nøst, E., 1994: Calculating tidal current profiles from vertically integrated models near the critical latitude in the Barents Sea. *J. Geophys. Res.,* **99** (C4), 7885–7901, doi:10.1029/93JC03485.

Phillips, O. M., 1977: *The Dynamics of the Upper Ocean.* 2nd ed. Cambridge University Press, 336 pp.

Starr, V. P., 1959: Hydrodynamical analogy to $E = mc^2$. *Tellus,* **11,** 135–138, doi:10.1111/j.2153-3490.1959.tb00013.x.

Stokes, G. G., 1846: Report on recent researches in hydrodynamics. *Rep. 16th Brit. Assoc. Adv. Sci.,* 1–20.

——, 1847: On the theory of oscillatory waves. *Trans. Cambridge. Philos. Soc.,* **8,** 441–455.

Sverdrup, H. U., 1927: *Dynamic of Tides on the North Siberian Shelf: Results from the Maud Expedition.* Vol. 4. Geofysiske Publikasjoner, 75 pp.

Ursell, F., 1951: Trapping modes in the theory of surface waves. *Math. Proc. Cambridge Philos. Soc.,* **47,** 347–358, doi:10.1017/S0305004100026700.

——, 1952: Edge waves on a sloping beach. *Proc. Roy. Soc. London,* **A214,** 79–97, doi:10.1098/rspa.1952.0152.

Weber, J. E. H., 2012: A note on trapped Gerstner waves. *J. Geophys. Res.,* **117** (C3), 30–48, doi:10.1029/2011JC007776.

——, and A. Melsom, 1993: Transient ocean currents induced by wind and growing waves. *J. Phys. Oceanogr.,* **23,** 193–206, doi:10.1175/1520-0485(1993)023<0193:TOCIBW>2.0.CO;2.

——, and P. Ghaffari, 2009: Mass transport in the Stokes edge wave. *J. Mar. Res.,* **67,** 213–224, doi:10.1357/002224009789051182.

——, and E. Støylen, 2011: Mean drift velocity in the Stokes interfacial edge wave. *J. Geophys. Res.,* **116,** C04002, doi:10.1029/2010JC006619.

——, and M. Drivdal, 2012: Radiation stress and mean drift in continental shelf waves. *Cont. Shelf Res.,* **35,** 108–116, doi:10.1016/j.csr.2012.01.001.

——, G. Broström, and Ø. Saetra, 2006: Eulerian versus Lagrangian approaches to the wave-induced transport in the upper ocean. *J. Phys. Oceanogr.,* **36,** 2106–2117, doi:10.1175/JPO2951.1.

——, K. H. Christensen, and C. Denamiel, 2009: Wave-induced setup of the mean surface over a sloping beach. *Cont. Shelf Res.,* **29,** 1448–1453, doi:10.1016/j.csr.2009.03.010.